



HAL
open science

Effects of humidity and glidants on the flowability of pharmaceutical excipients. An experimental energetical approach during granular compaction

M.-G. Cares Pacheco, M.-C. Jiménez Garavito, A. Ober, F. Gerardin, E. Silvente, V. Falk

► To cite this version:

M.-G. Cares Pacheco, M.-C. Jiménez Garavito, A. Ober, F. Gerardin, E. Silvente, et al.. Effects of humidity and glidants on the flowability of pharmaceutical excipients. An experimental energetical approach during granular compaction. *International Journal of Pharmaceutics*, 2021, 604, pp.120747. <10.1016/j.ijpharm.2021.120747>. <hal-03731392>

HAL Id: hal-03731392

<https://hal.univ-lorraine.fr/hal-03731392v1>

Submitted on 13 Jun 2023

HAL is a multi-disciplinary open access archive for the deposit and dissemination of scientific research documents, whether they are published or not. The documents may come from teaching and research institutions in France or abroad, or from public or private research centers.

L'archive ouverte pluridisciplinaire **HAL**, est destinée au dépôt et à la diffusion de documents scientifiques de niveau recherche, publiés ou non, émanant des établissements d'enseignement et de recherche français ou étrangers, des laboratoires publics ou privés.



Distributed under a Creative Commons CC BY-NC 4.0 - Attribution - Non-commercial use - International License

1 Effects of humidity and glidants on the flowability of 2 pharmaceutical excipients. An experimental energetical approach 3 during granular compaction

4 M.-G. Cares Pacheco^{*1}, M.-C. Jiménez Garavito^{1,2}, A. Ober¹, F. Gerardin², E. Silvente²,
5 V. Falk¹.

6 1. University of Lorraine, CNRS, LRGP, F-54000 Nancy, France

7 2. Department of Process Engineering, French National Research and Safety Institute for
8 the Prevention of Occupational Accidents and Diseases, 54519 Vandœuvre, France.

9 Abstract

10 Granular materials are part of the design, production and final products of different industrial sectors. Powder
11 flowability is a major topic in manufacturing and transport as it is closely related to process feasibility. Nonetheless,
12 the flows of granular materials are not easy to describe or quantify, even in the simple case of dry monodisperse
13 cohesionless particles. Flowability assessment is not a standard or normalized issue; still, no test is able predict
14 powder flow behavior in all the different mechanical situations encountered during processing.

15 This study aims (1) to evaluate flowability, as device-related, through the force or the energy supplied to the powder
16 bed and (2) to study the effect of glidants and moisture content on flowability. To illustrate these aims, the flowability
17 of two well-known pharmaceutical excipients, Avicel[®] PH-102 and Retalac[®] mixed with four different types of
18 precipitated nano-silica (SIPERNAT[®] D10, D17, 50 S and 500 LS), was assessed using two granular compaction
19 devices: Densitap[®] and FT4[®] compaction cell. Our results show that the hydrophilicity of colloidal silica affects
20 surface coverage, ranging from 6% to over 80%. Binary mixtures with hydrophobic additives, D10 and D17, generated
21 smaller silica aggregates with a wider spread on the surface of host particles. For Retalac[®] conditioned at 20% RH,
22 HR values changed from 1.30 (acceptable flow) to 1.17 (good flow). For Avicel[®] PH-102, conditioned at 60% RH,
23 HR values changed from 1.22 (fair flow) to less than 1.10 (excellent flow).

24 1 Introduction

25 Those who work with granular materials, fine or coarse, such as powders, know that the same
26 powder may flow well in one container but poorly in another. Despite all the available studies
27 describing flow characteristics, it is often difficult to extract common features and general trends
28 for granular materials that are not glass beads. Granular flow complexity is related to its
29 multidimensional character as it links the local particle interactions and their global mechanical
30 behavior, including bulk properties, equipment design, processing conditions, and environmental
31 conditions. The difficulties and limitations of flow behavior assessment have been well-reviewed
32 (Prescott and Barnum, 2000; GDR MiDi, 2004; Schulze, 2008; Saker et al., 2019). To better
33 understand granular-flow behavior, it seems fundamental *to differentiate powder flow, as an*
34 *observation, from powder flow quantification* related to the assessment method, also known as

35 *flowability*. Flowability is device-dependent, and describes the ability to flow in a desired manner in
 36 a specific piece of equipment (Prescott and Barnum, 2000; Saker et al., 2019). Different parameters
 37 or indexes can be obtained from the multiple flow testers available on the market. Each one of
 38 these devices "estimates/quantifies" flowability under specific mechanical conditions. Still, no one
 39 test will predict powder flow behavior in all the different mechanical situations encountered during
 40 processing and transport. In practice, whether in the laboratory or during the manufacturing
 41 process, from know-how or through measurements, the type of test method that describes the best
 42 flowability in a given application is chosen.

43 Densification, or compressibility, or compactness, is a flow property arising from the collective
 44 forces acting on the media. When energy is transferred into a granular material, the grains begin
 45 to reorganize themselves in a denser structure. This energy can be transmitted to the powder bed
 46 using uniaxial compression or vibration. Generally, during uniaxial compression, particles undergo
 47 elastic, plastic, or visco-elastic/visco-plastic deformation. Softer solicitations, such as vibrations,
 48 give rise to the geometric rearrangement of particles. Compaction by vibration can be divided by
 49 subjecting the granular system to harmonically driven motions (Saker et al., 2019) or to free-falls
 50 performances, commonly denoted as tapping (Yu and Hall, 1994).

51 Several studies focus on the densification of granular media because it covers many fields from
 52 pharmaceuticals to Geotech industries (Rondet et al., 2017). As there is no universal mathematical
 53 model to predict flow behavior in every situation, the dynamics of compaction under vibration have
 54 been described by several empirical or heuristic models, mostly using glass beads (Knight et al.,
 55 1995; Head, 2000; Ribière et al., 2005; Yu and Hall, 1994). In this work, we will simply validate
 56 whether two of the most used models fit the dynamic behavior of two excipients, widely used in
 57 the pharmaceutical industry.

58 The first and the most famous model is the one proposed by Knight et al. (1995) from the James
 59 Frank Institute at the University of Chicago (Knight et al., 1995):

$$\rho(N) = \rho_f - \frac{\Delta\rho}{1 + B \ln(1 + \frac{N}{\tau})} \quad (1)$$

60 where N is the number of taps, ρ_f is the final compactness, $\Delta\rho$ is the difference compared to
 61 the initial compactness of the bed, while the B and τ parameters are defined as a function of the
 62 acceleration, the control parameter.

63 The first term shows the rapid arrangement of the particles, while the second expresses that the
 64 steady state is reached asymptotically, logarithmic slow (Ribière et al., 2005). This also indicates
 65 that grains behave in a manner similar to glass (Head, 2000).

66 The densification of dry granular materials by tapping is often better fit by an empirical law
 67 developed by Kohlrausch-Williams-Watts (KWW model), (Yu and Hall, 1994):

$$\rho(N) = \rho_\infty - \Delta\rho \cdot \exp\left(-\left(\frac{N}{\tau}\right)^\beta\right) \quad (2)$$

68 where ρ_∞ is the compactness at the steady state, τ is the characteristic relaxation time describing

69 the arrangement of grains until the steady state is reached and β is the stretching exponent.

70

71 From a technological point of view, powder flow is essential to processing efficiency. The aim is
72 to facilitate manufacturing, including flow through hoppers, sieving, pouring, blending, transport,
73 filling, compaction and tableting, even if this rarely brings an added value to the end-use product.

74 The flowability of cohesive powders can be remarkably improved by the use of flow additives or
75 glidants (Valverde, 2013). For several years, flow regulators have been systematically added to
76 a significant number of formulated products, without any studies validating its function besides
77 process feasibility. In the pharmaceutical industry, the use of glidants is mostly based on historical
78 know-how or trial error methods, without any measurements of the effect on end-use properties
79 (Majerová et al., 2016).

80 Amorphous silica powders (NP-SC) were introduced quite easily under the hypothesis that only
81 crystalline silica is considered a toxic form at a micrometric scale. Nonetheless, some recent risk
82 assessment studies carried out at the National Institute of Scientific Research in France (INRS)
83 demonstrated the in-vitro cytotoxicity of amorphous silica, which is also highly incremented by
84 reducing the size of the particles (Ricaud, 2007). Therefore, it is crucial to focus on the role of
85 silica nanoparticles on the end-use properties of powders, especially on their flowability, to optimize
86 the choice of additives, minimize their quantity, or to replace them. Nevertheless, to do so, it is
87 essential to better understand how they interact within the formulations/media into which they
88 are added.

89 Different flow regulator action mechanisms have been proposed in the literature. The first is related
90 to a purely mechanical effect, and the second is related to interparticle forces. A mechanical effect
91 will occur when surface additives allow particles to easily roll over one another, thus reducing
92 friction (Duran Jacques, 1997). The physical mechanism by which interparticle adhesive forces
93 are reduced is less exact, or at least not universal. When referring to interparticle forces, two
94 mechanisms have been proposed. The first is related to surface chemistry changes, and the second
95 concerns spacers among host particles (Quintanilla et al., 2006; Fulchini et al., 2017; Ruzaidi et al.,
96 2017).

97

98 The aims of this work are (1) to obtain a deeper understanding of how granular compaction is
99 related to flow behavior by confronting different compaction tests, thus pointing out a standard
100 physical parameter: the specific energy supplied to the powder bed; (2) to study the effect of
101 glidants and environmental moisture conditions on flowability.

102 To illustrate these aims, granular compaction was performed using two compaction devices: the
103 well-known DensiTap[®] and the FT4 compression module. Measurements were carried out in the
104 elastic domain, using two pharmaceutical excipients, lactose and microcrystalline cellulose. Several
105 different types of precipitated nano-silica were used as surface additives, differentiated by their
106 hydrophilicity and size distribution. Powder flowability was determined, or classified, according to
107 the Hausner ratio (HR), a widely used index in the industry (Saker et al., 2019).

108 2 Materials and methods

109 2.1 Powder Materials

110 Excipients as host powders

111 For this study, two well-known pharmaceutical ingredients with excellent compactibility were
112 chosen: Avicel[®] PH-102 and RetaLac[®]. Avicel[®] PH-102 is a high purity microcrystalline
113 cellulose produced by FMC Biopolymer[©] (United States), generally used in the pharmaceutical
114 industry to tableting by direct compression. The RetaLac[®] is a co-processed hypromellose/lactose-
115 based excipient produced by MEGGLE (Germany), composed of equal parts of a K-type
116 hypromellose polymer and α -lactose monohydrate. RetaLac[®] excipient is specifically designed
117 for direct compression and dry granulation of modified release formulations.

118 Nanoparticles as flow regulators

119 The SIPERNAT[®] brand from Evonik (Germany) was chosen for flow regulation in bulk powders.
120 SIPERNATs are highly porous colloidal silicon dioxide powders produced by precipitation from an
121 aqueous solution. From the large panel of SIPERNAT[®] NPs, two with hydrophobic properties,
122 D10 and D17, and two hydrophilics, 50 S and 500 LS, were chosen. Both D10 and D17 are rendered
123 hydrophobic by a chemical surface treatment. D10 is used in a wide variety of defoamer while D17
124 primary application is as an anticaking agent in fire extinguishing powders. 50 S and 500 LS
125 products are high absorption capacity carriers, able to absorb liquids up to three times of their
126 own mass. The 50 S is normally used in plant formulations, such as wettable powders and water-
127 dispersible granules. The 500 LS is recommended as a viscosity modifier in liquid systems and flow
128 aid and anti-caking agents for fine powders.

129 Sample conditioning

130 All samples were conditioned and maintained at room temperature, inside sealed containers
131 controlled by saturated salt/water solutions to control relative humidity at 20% (Magnesium
132 chloride - MgCl₂) and 60% (Sodium Chloride - NaCl). Samples equilibrate until they reached
133 the environment conditions, validated by daily water activity, a_w , measurements using an Aqualab
134 4TE from METER[®].

135 To study the surface additives' influence on flowability, bulk powders were weighed with 0.5 and 2%
136 w/w for each flow regulator and blended in a 3D shaker mixer Turbula[®] T2F from the WAB group
137 for 20 minutes. It should be noted that no differences in flowability assessment were obtained when
138 the mixing time increased from 10 to 60 minutes. Once the mixtures were made, samples were
139 conditioned and maintained at room temperature, inside sealed containers controlled by saturated
140 salt/water solutions as described above.

141 2.2 Physical characterization techniques of powders

142 Particle size distributions were measured by laser diffraction in liquid media with a Mastersizer
143 2000 from Malvern Instruments. Ethanol was used in order to improve particle dispersion and
144 to avoid dissolution. All samples were analyzed in triplicate to ensure reproducibility, with an

145 instrument uncertainty of 1 [μm].
 146 Particle morphology analyses were assessed with a JSM T330A Scanning Electron Microscopy
 147 (SEM) from JEOL, and a field emission gun operating at 5 kV. Before analysis, samples were
 148 placed onto doubled-sided adhesive and coated with Gold-Palladium mixtures for 6 minutes using
 149 an Ion SPUTTER JFC-1100 under an air purge. Particles/glidants mixtures were analyzed with
 150 a Field Emission SEM from ZEISS Merlin Compact with the proven GEMINI I electron column.
 151 Samples were placed onto carbon conductive tape and coated with about 20 nm of carbon. EDS
 152 analyses were performed with a QUANTAX-XFlash6 detector with a peak resolution of 129eV,
 153 from Bruker. EDS was performed to confirm the presence of colloidal silicas on the surface of host
 154 powders.

156 Water sorption isotherms were performed at 20°C in 3 Flex from Micromeritics. Before scanning,
 157 samples were vacuum dried for ten hours at 15° C. The true density analysis of powder was performed
 158 in an AccuPyc 1330 Helium pycnometer from Micromeritics. All data measurements are the average
 159 of ten measurements obtained from one powder sample.

160 2.3 Granular compaction devices

161 Vibration, free surface conditions

162 To determine flowability from tapped density measurements, different methods and devices can be
 163 used. The most used, described on the United States Pharmacopoeia, suggests freely pouring a test
 164 sample weight of 100 g in a 250 mL volumetric cylinder as shown in Fig. 1. The protocol consists
 165 of measuring the unsettled apparent volume, V_0 , and carrying out 10, 500, and 1250 taps on the
 166 same powder sample and reading the corresponding volumes to the nearest graduated unit. If the
 167 difference between V_{500} and V_{1250} is less than or equal to 2 mL, V_{1250} is the tapped volume. If the
 168 difference between V_{500} and V_{1250} exceeds 2 mL, repeat in increments of V_{1250} , until the difference
 169 between succeeding measurements is less than or equal to 2 mL (Pharmacopeia, 2015).

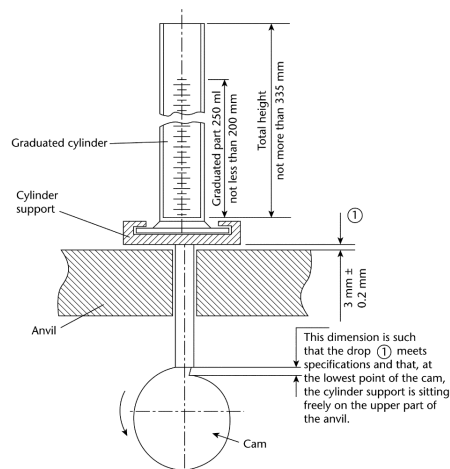


Figure 1: Apparatus description from Pharmacopeia (2015).

170 In this study, DensiTap[®] from Granuloshop[©] was used for measuring bulk density with a graduated

171 glass cylinder of 250 mL. In this device, the tapping action is provided, under zero shear conditions,
172 by a rotating cam that raises the cylinder platform through a fixed distance of 3 mm at a nominal
173 rate of 250 drops per minute. About 150 mL of powder was freely poured using a funnel into the
174 vessel allowing the aerated density to be determined. It should be noted that it is impossible to fit
175 100 g of Avicel[®] PH-102 or RetaLac[®] in a 250 mL container; this is similar for a wide range of
176 pharmaceutical excipients.

177 Several authors suggest that flow behavior analysis using tapped density data is strongly affected by
178 the highly irreproducible initial pouring of the powder. As described in previous works, Saker et al.
179 (2019), we found a highly reproducible initial state when controlling powder moisture conditioning.
180 Thus, the data error was determined by considering systematic and random errors, and to do so,
181 each experiment was repeated 3 times.

182 Uniaxial compaction, packed bed conditions

183 Compressibility studies in packed bed conditions were performed using an FT4 powder rheometer
184 from Freeman Technology[®]. The samples were poured into a borosilicate split vessel. The test
185 started with a mechanical conditioning step by establishing uniform stress in the powder bed (Fig.
186 2, left). When the conditioning cycle is over, the vessel splits allowing a precise volume of 10 mL
187 to be attained. The analysis was achieved by applying increasing levels of force directly onto the
188 granular media with a vented piston, allowing the trapped air within the powder to escape, and by
189 measuring volume changes depending on the applied load (Fig. 2, right).

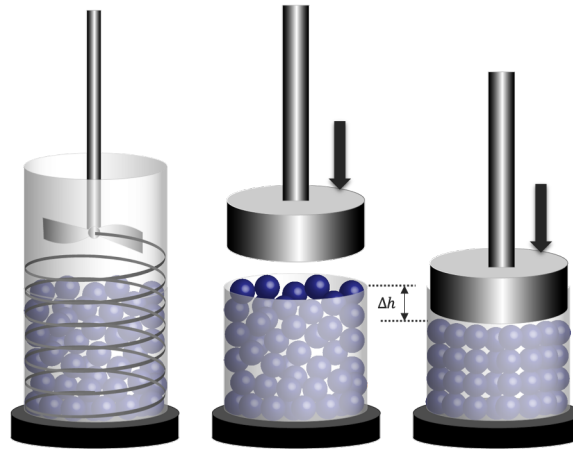


Figure 2: FT4 rheometer compressibility test, from conditioning to compaction.

190 During the test, the changes in volume for a given applied normal stress were collected. In order
191 to determine the specific energy supplied to the granular media an external data treatment must
192 be carried out. In fact, FT4 software determines the energy supplied to the powder by using a
193 trapezoidal numerical integration. Nevertheless, this data treatment lacks of physical meaning as
194 it integrates all height changes, even the non-decreasing ones. As the height sensor is extremely
195 sensitive, the energy provided to the system is calculated as time-dependent and so, aberrant
196 values can be obtained. In order to give a mechanical sense to the experimental data, the specific
197 energy supplied to the system was determined with Matlab[®] by discretizing the normal stress

198 values as function of the packed bed height evolution. To do so, it is necessary to identify the areas
 199 where the normal stress is kept constant by the derivative of force with respect to time (Fig. 3.a
 200 in red). Then, to determine an average force, and to be able to relate it to displacement values,
 201 we selected around 20 data values in the red zone, where non-evolution was found. Finally, each
 202 setpoint gave rise to a specific energy value which is related to HR as shown in Fig. 3b.
 203

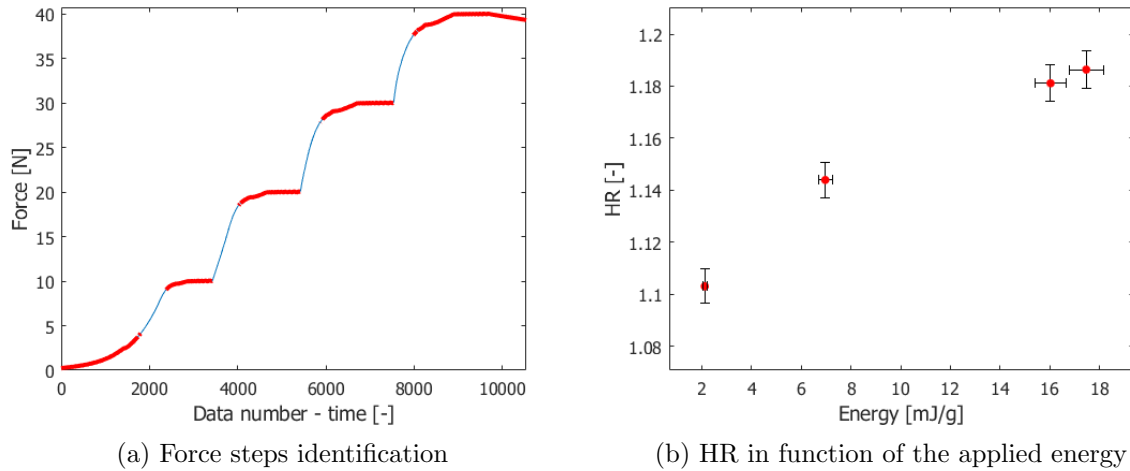


Figure 3: Example of FT4 compaction test data treatment. Applied normal stress increments of 10 N until 40 N.

204 To allow a better comparison between the devices, their characteristics and operating conditions
 205 are summarized in Table 1. It should be noted that powder humidity conditioning and control
 206 allowed us to obtain a highly reproducible initial state, regardless of the device. This argument
 207 allowed us to validate the use of HR as a flow behavior index, others could be used (Carr, Void
 208 ratio).

Table 1: Device characteristics

Characteristics/Device	Densitap	FT4
Compaction by	vibration: Free falls	Normal stress
Particles reorganization	Free surface	Packed bed
Scanning	Number of taps	Force [N]
Quantity of powder [mL]	150	10
Vessel material	borosilicate glass	borosilicate glass
Applied Force [N]	215	0 - 40
Vessel dimensions [mm] (diameter/height)	26/300	25/30

3 Results & Discussion

3.1 Physical characterization

The particle size distribution analysis, summarized in Table 2, shows that Avicel PH-102 particles are bigger than Retalac. From the SEM images, scale bar of 100 μm and 500 μm , Avicel[®] PH-102 particles exhibit an isometric rod shape with a rough surface (Fig. 4), while Retalac[®] seems to be composed of agglomerates of amorphous-like particles (Fig. 5). Absorption/Desorption isotherms showed that both excipients are hydrophilic and absorb water at low moisture content (Fig. 6). Samples' sorption behavior analyses determined our moisture conditioning choice, 20 and 60% RH.

Table 2: Excipients as host particles

Powder	Particle size distribution ± 1 [μm]					Behavior towards water **
	d_{10}	d_{50}	d_{90}	d_{32}	d_{43}	
Avicel [®] PH-102	29	104	248	40	126	Hydrophilic
RetaLac [®]	89	203	408	159	229	Hydrophilic

Some of the physical characteristics of the silica nanoparticles are shown in Table 3. Supplier size specifications describe micro-size particles/aggregates using laser diffraction. The European Commission proposes that materials can be classified as nanomaterials (NM) if their volume-specific surface area, VSSA, is larger than 60 m^2/cm^3 (Rauscher et al., 2019). Thus, according to the VSSA estimations, SIPERNATs D10, D17, 50S and 500LS can be considered as NMs.

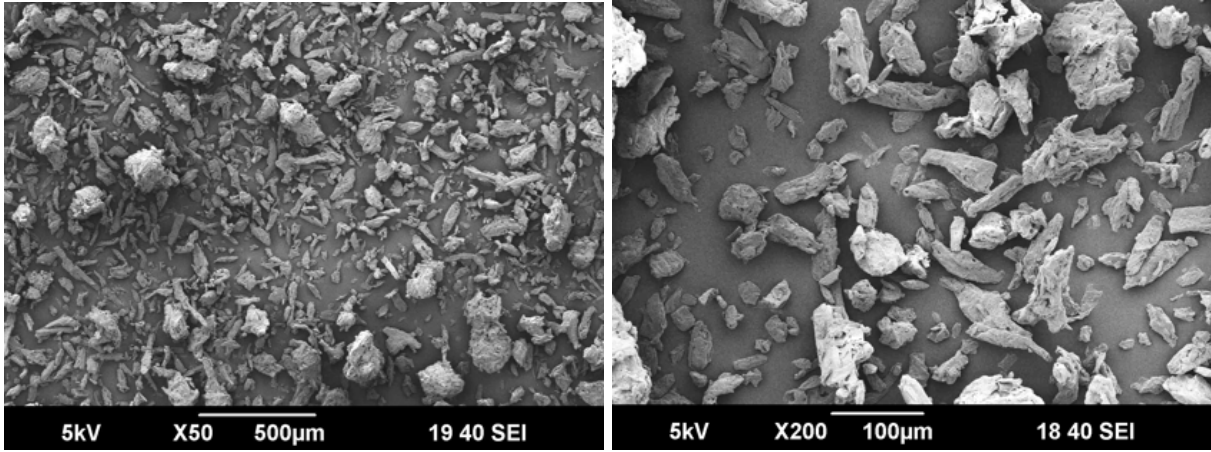


Figure 4: SEM micrographs of Avicel[®] PH-102, at different magnifications.

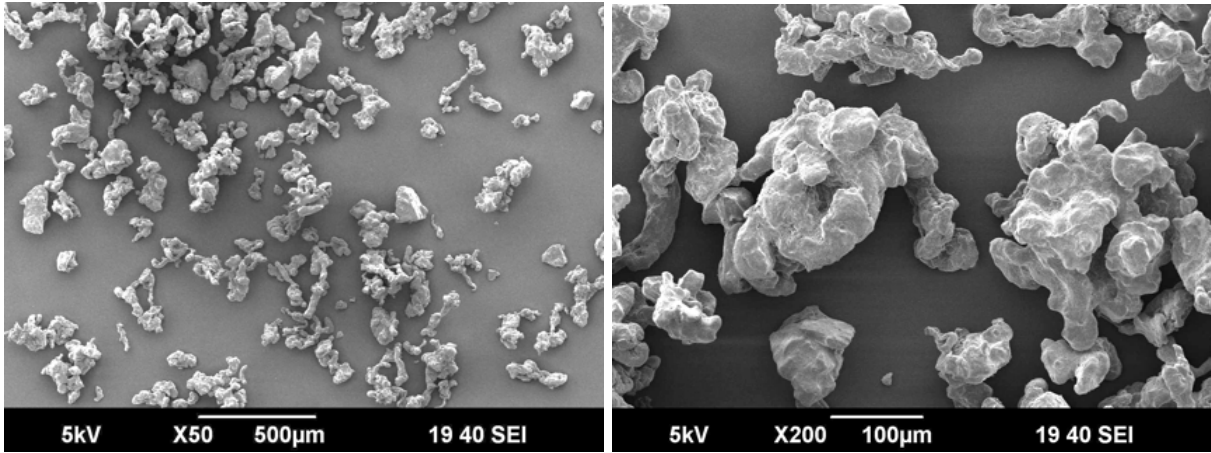


Figure 5: SEM micrographs of RetaLac[®], at different magnifications.

Table 3: Physical characteristics of silica nanoparticles

SIPERNAT	Particle size distribution			BET ** [m^2/g]	VSSA* [m^2/cm^3]	Behavior towards water **
	d_{50}^{**}	d_{50}^*	d_{32}^*			
D10	6.5	7	7	90	178	Hydrophobic
D17	10	8	6	100	201	Hydrophobic
50 S	18	16	14	500	1060	Hydrophilic
500 LS	10.5	14	12	450	968	Hydrophilic

** Evonik data, * our data, both in [μm]

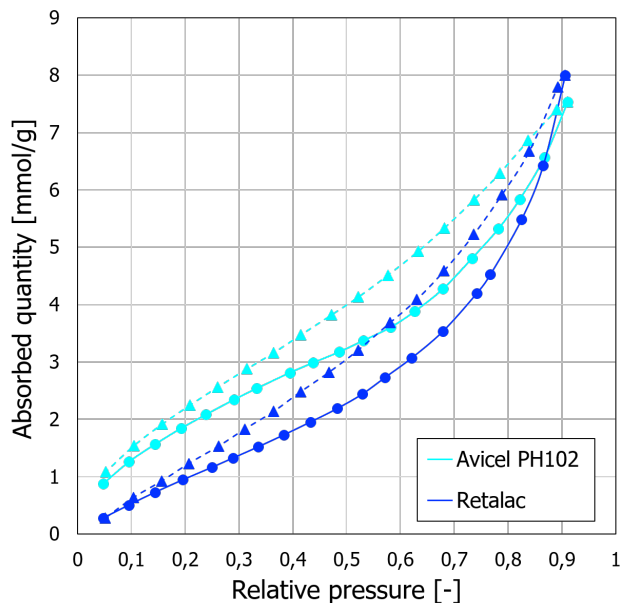


Figure 6: Water sorption isotherms of Avicel[®] PH 102 (cyan) and Retalac[®] (blue), at 20°C. Sorption curves are represented with a solid line, and desorption curves with a dashed line.

222 3.2 Dynamics of compaction under free surface conditions

223 The evolution of powders compactness during vibration according to the number of taps is presented
 224 in figure 7. As expected, poorly flowing powders, such as Avicel[®] PH-102, are more compressible.
 225 Also, the repeatability from 3 experiments showed a larger random error using Retalac[®], despite
 226 the conditioning (Fig. 7).

227 It is common use in scientific literature to determine tapped density systematically after 500 taps,
 228 as the number of taps suitable to reach the steady state (Traina et al., 2013). For Avicel[®] PH-102
 229 at 500 taps, the powder bed had not reached its maximal compaction state and so, the HR value
 230 obtained at this state (or time) is significantly different from the one obtained after 10 000 taps
 231 (Fig. 7.a). Using HR_{500} Avicel[®] PH-102 flowability is classified as "Acceptable", while at 10
 232 000 taps is classified as "Cohesive", which is consistent with its flow behavior observed with the
 233 naked eye. In difference, for RetaLac[®] samples, there is not a significative evolution of the powder
 234 compactness after 500 taps (Fig. 7.b).

235 It should be noted that both samples exhibit an easily reproducible initial state regardless the
 236 moisture content. Moreover, the moisture content at 20% or 60% RH has no influence on samples
 237 compaction when using Densitap as a flow tester (Fig. 8).

238 Modeling

239 The mathematical model describing the dynamic of compaction showed a similar fit for the Chicago
 240 and the KWW model with, in both cases, at least a 97% prediction interval (Figs. 9 and 10). The
 241 limitation of the Chicago model lies in the fact that it does not fit the experimental data when

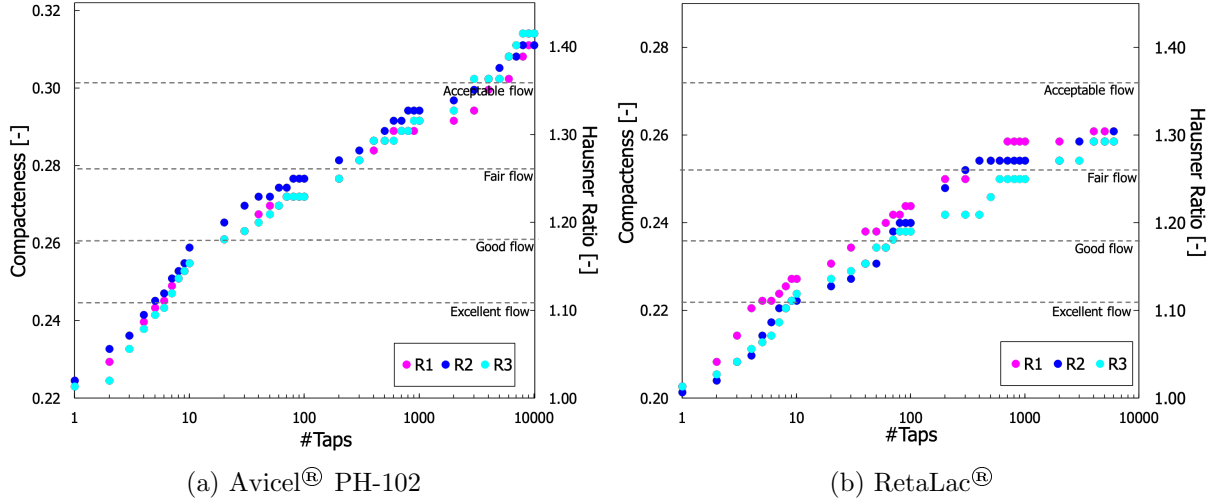


Figure 7: Study of the dynamic of compaction in DensiTap[®] samples conditioned at 20% RH.

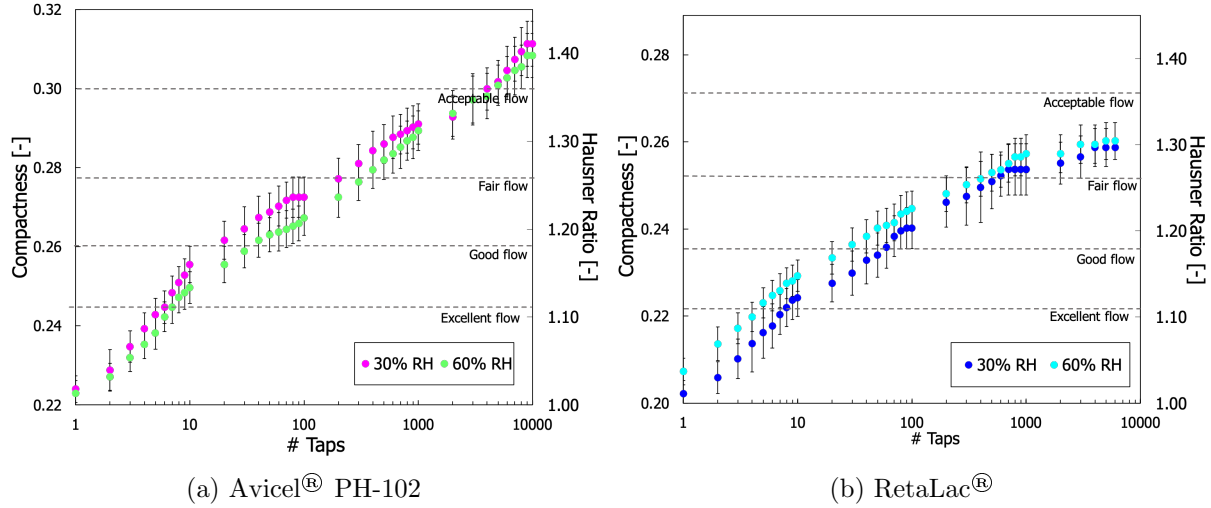
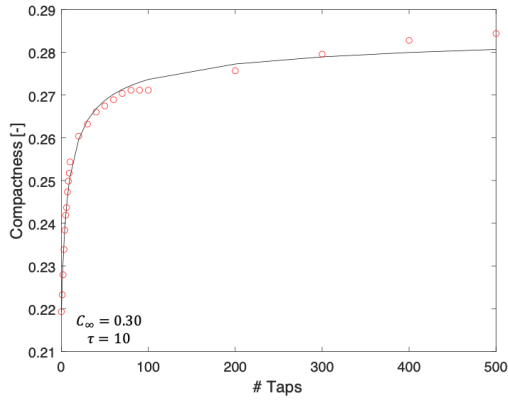


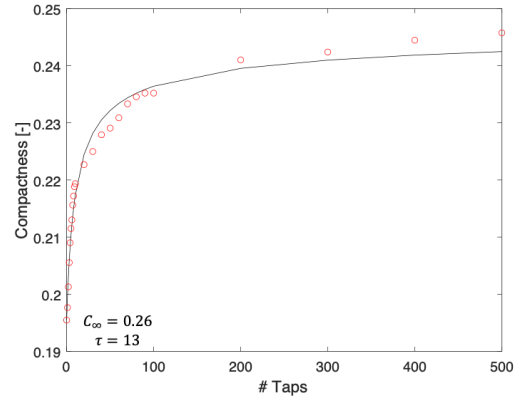
Figure 8: Dynamic of compaction as function of the powder moisture content using DensiTap[®]

242 approaching the stationary state (Fig. 9). Thus, it fails to predict the number of taps needed to
 243 reach the steady state, τ . For example, for Avicel[®] PH-102 the predicted number of taps needed to
 244 reach the steady state was around 100 000 taps while experimentally, only 8 000 taps are required.
 245 Nevertheless, the ρ_∞ parameter obtained from the model is predicted fairly accurately. For ex
 246 ample for Avicel[®] PH-102 $\rho_\infty = 0.29 \pm 0.01$, while experimental data showed a $\rho_\infty = 0.31 \pm 0.01$.

247 In the KWW model, ρ_f is used as a minimization parameter better fitting the experimental
 248 data when reaching the steady state. In this case, the value of τ -parameter, seems to be more
 249 representative of the progressive arrangement of grains. Nonetheless, a slight deviation from the
 250 model is detected for the first 40 taps (Fig. 10). Similar results were obtained for the samples
 251 conditioned at 60% RH.

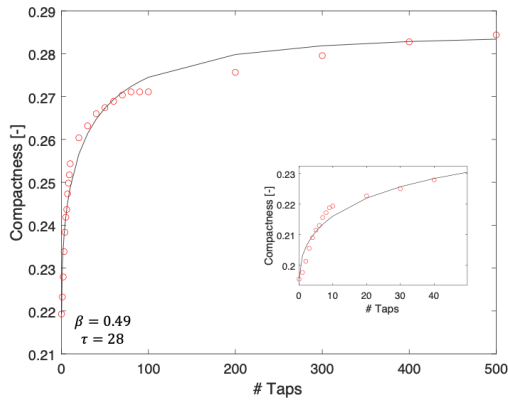


(a) Avicel[®] PH-102

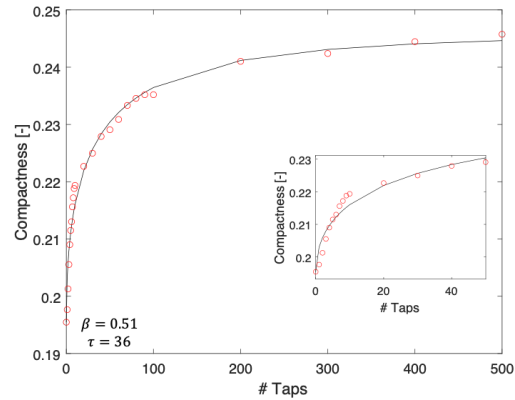


(b) RetaLac[®]

Figure 9: Chicago Model obtained from iterative minimization using DensiTap data (500 taps). Samples conditioned at 20% RH.



(a) Avicel[®] PH-102 - 500 taps



(b) RetaLac[®] - 500 taps

Figure 10: KWW model obtained from iterative minimization using DensiTap data (500 taps). Samples conditioned at 20% RH.

252 The mathematical model describing the dynamic of compaction showed a similar fit for the Chicago
 253 and the KWW model with, in both cases, at least a 97% prediction interval (Figs. 9 and 10). Rondet
 254 et al. (2017) compared different densification models highlighting that the KWW equation ensures
 255 the best mathematical fitting of the experimental data using R^2 as a fit parameter. This statement
 256 is accurate for powders such as Kaolin and Calcium phosphate. Nonetheless, when they analyzed
 257 unsaturated microcrystalline cellulose, the authors found a better agreement between the KWW
 258 and Chicago model, which agrees with our results. Differences can also arise from the use of R^2 ,
 259 as an inadequate parameter to determine the goodness of fit for nonlinear models.

260 3.3 From compressibility to flowability, an energetic approach

261 In this section, we study flowability from compressibility as a function of the consolidation strength.
 262 To do so, each applied load gives rise to a steady compaction state that can be related to the HR
 263 value. In order to study the energy impact, we tested four different ramps of force from 2 to
 264 40N. Some of the results are shown in figure 11.a using Avicel[®] PH-102 conditioned at 60% RH.
 265 As shown in the figure, powder compactness and flowability evolve exponentially with the specific
 266 energy supplied to the powder bed.

267 Compressibility is surprisingly independent of the force ramp step, meaning that the powder's
 268 previous mechanical history does not influence its compaction behavior. We always obtained the
 269 same compaction state for a given energy, indifferent to previous loads. To deepen such a statement,
 270 we decided to study the influence of the conditioning step, which intends to provide a reproducible
 271 initial state by subjecting the samples to the same mechanical treatment, acting as an aeration
 272 phase. Two force ramps were tested with and without the conditioning step. Results in figure 11.b
 273 showed no significant difference between the samples subjected to mechanical conditioning and the
 274 simple act of freely pouring the powder. In this case, compressibility, and so flowability, seemed to
 275 only be affected by the maximal load supplied to the granular media.

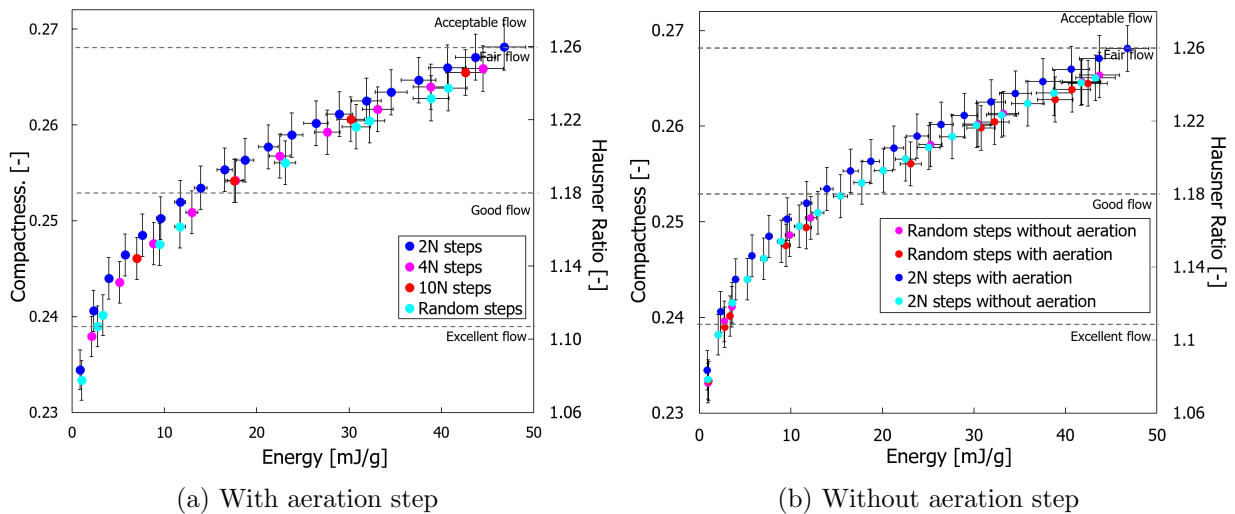


Figure 11: FT4 compaction test at different force ramps with Avicel[®] PH-102 at 60% RH.

276 The effect of moisture content on compactness, and so on flowability, is presented in Figure 12.
 277 For Avicel[®] PH-102, the sample conditioned at 20% RH had a better flowability than the one
 278 conditioned at 60% RH, despite the specific energy supplied to the media (12.a). It is well-known
 279 that the moisture content in granular media favors the formation of liquid bridges, thus increasing
 280 particle cohesion and decreasing flowability. Notwithstanding, for Retalac, moisture content seems
 281 to not have any influence on its flowability.

282 Avicel[®] PH-102 results are in contradiction with those obtained with DensiTap[®] (Fig. 8.a). Unlike
 283 Densitap, the compression test allows a good differentiation of the two environmental conditionings.
 284 The strength of the applied load could explain this. Densitap[®] transfer a force of about 215 N to
 285 the granular media, while in FT4 experiments the maximal load is about 40 N. At low applied forces,

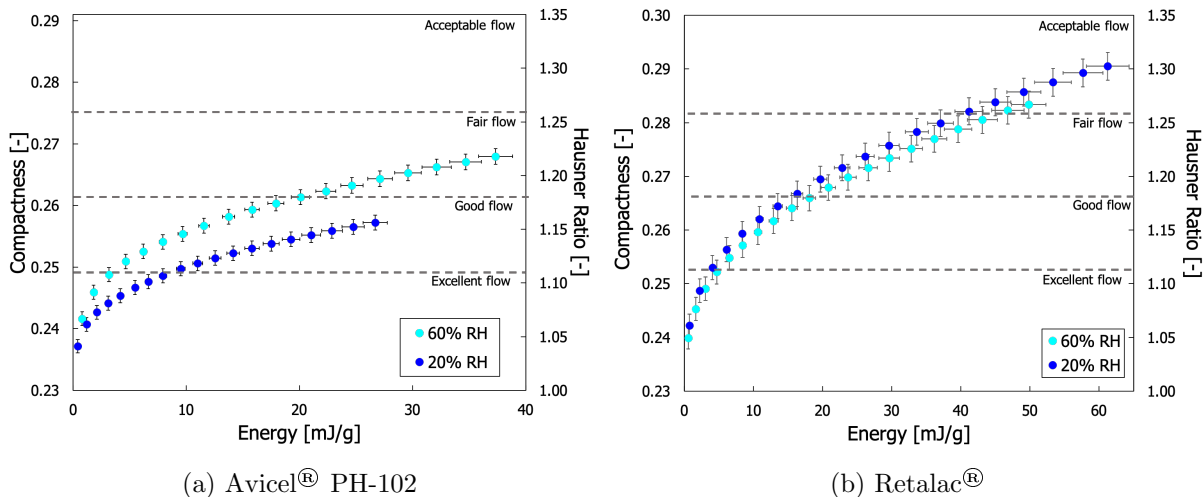


Figure 12: Compactness and flowability assessment as a function of the specific energy supplied to the system. Samples conditioned at 20% and 60% RH.

286 like those provided by the FT4 compaction cell, some granular materials, more precisely cohesive
 287 powders, such as Avicel[®] PH-102, will not reach a high compaction state (Fig. 13). For example,
 288 in this case, using FT4 and Densitap, the flowability could be described as *Good* to *Fair*, with *Fair*
 289 being more appropriate for the real flow behavior of the powder. On the contrary, Retalac[®] samples
 290 can be classified as having an *Acceptable flow*, regardless of the device. In summary, FT4 results
 291 describe flowability during uniaxial compression at low consolidation strength, and so, powder flow
 292 properties could differ for higher consolidation stress as shown in figure 13. The energetic approach
 293 allows us to understand the differences, or similarities, in flowability assessment when comparing
 294 devices.

295 3.4 Colloidal silicas as glidants

296 Both host powders were weighed with 0.5 and 2% w/w of SIPERNAT[®] 50S, 500LS, D10 and
 297 D17 (Figs. 14 and 15). For binary Retalac mixtures conditioned at 20% RH, all the configurations
 298 studied, in terms of the type of glidant and concentration, significantly improved powder flowability
 299 (Fig. 14.a). In contrast, no statistically significant differences were obtained between flow
 300 regulators. The increase in moisture content of binary mixtures at 60% RH showed similar results
 301 (Fig. 14.b). In the case of Avicel[®] PH-102, the four NPs used in our study, D10, D17, 50S
 302 and 500LS, significantly improved the flowability of the host particles regardless of the moisture
 303 content (Figs. 15 and 16). Firstly, no statistically significant differences between NPs with the
 304 same behavior towards water were found (Fig. 15.a). Secondly, no differences were obtained when
 305 increasing the amount of NPs added to the host particles, independent of its hydrophilic nature
 306 (Fig. 15.b).

307 In summary, the effect of adding 0.5% w/w of SIPERNAT[®] D10 or 500 LS, on Avicel[®] PH-
 308 102 flowability at different moisture conditions is presented in figure 16. In this case, despite
 309 the moisture content, both glidants, D10 and 500LS, improved significantly the flowability of the

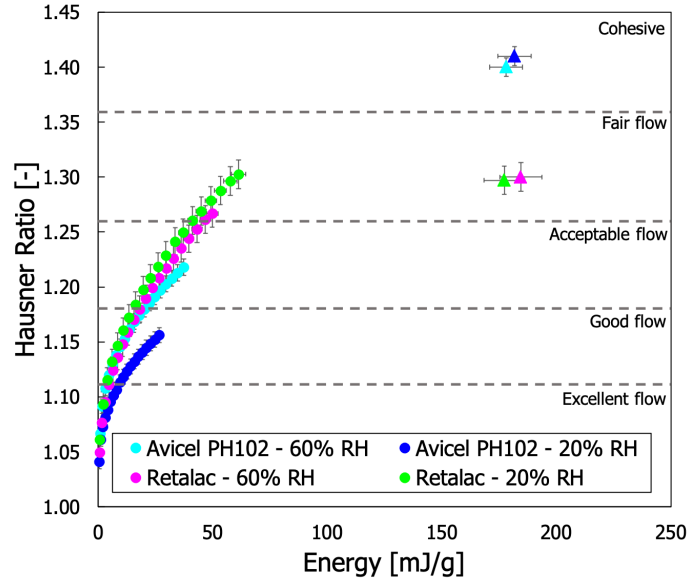


Figure 13: Flowability assessment as function of the specific energy supplied to the granular media using FT4 (circles) and Densitap (triangles) devices.

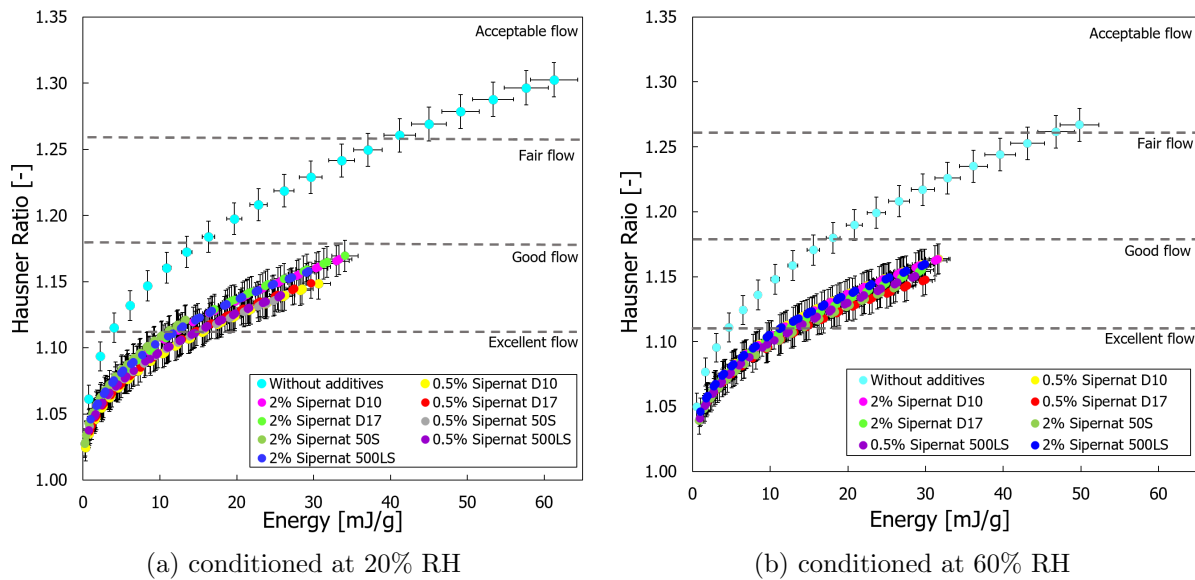


Figure 14: Flow influence of NPs for RetaLac[®] using FT4. Force ramp from 0 to 40 N using a 2 N step.

310 excipient, with a better performance of the hydrophobic one, D10. Similar results were obtained by
 311 Müller et al. (2008). In their work, the authors observed, using binary mixtures of corn starch,
 312 that hydrophobic flow regulators reduce cohesive forces to a greater extent than hydrophilic ones.
 313 Ruzaidi et al. (2017) also showed that hydrophobic nano-silica improved ibuprofen's flowability
 314 slightly more than the hydrophilic one. In comparison, Zimmermann et al. (2004) did not find any

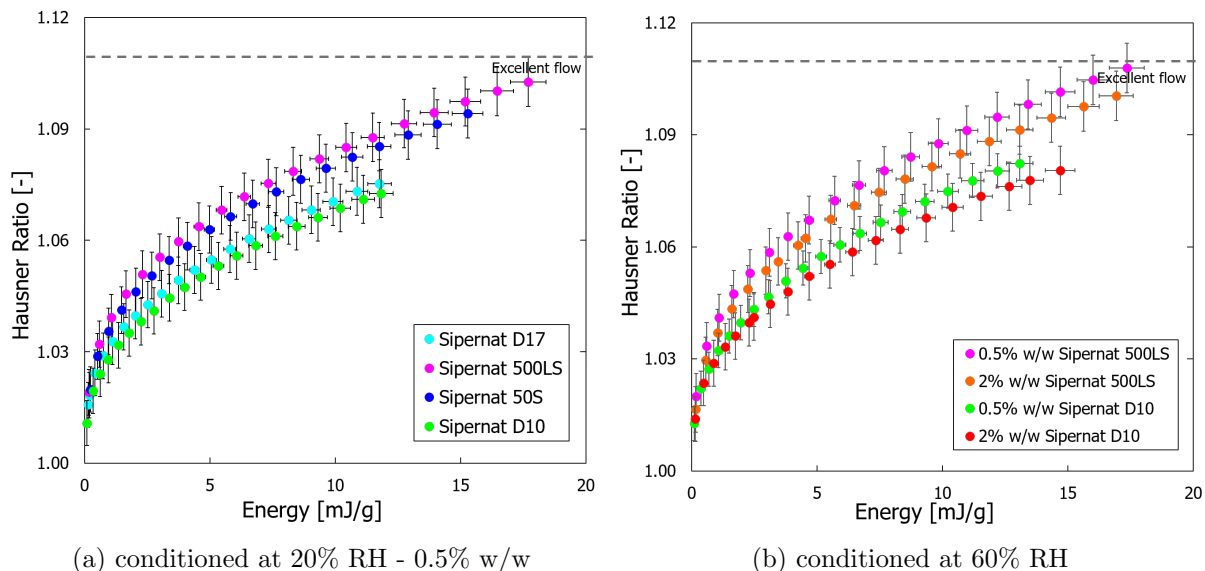


Figure 15: Flowability influence of NPs for Avicel[®] PH-102 using FT4. Force ramp from 0 to 40N using a 2N step.

315 direct correlation between the hydrophilicity of the nanomaterials (fumed nano-silica, Aerosils[®])
 316 and their ability to reduce the tensile strength of powder mixtures with corn starch.

317 Several hypotheses could explain this behavior. The first one is related to surface chemistry changes.
 318 As Avicel[®] PH-102 is highly hydrophilic, its surface modification may reduce the liquid bridge
 319 formation during moisture conditioning. The second one is related to the size of the additives.
 320 Kojima and Elliott (2012), using binary mixtures of polymer powder with Aerosils[®] , showed that
 321 the smaller the size of the colloidal silica and their aggregates, the more effectively they worked as
 322 lubricants, thus reducing internal friction. Similar results were obtained by Müller et al. (2008), who
 323 worked with binary mixtures at 0.2% w/w. Nonetheless, in our case, when comparing SIPERNAT[®]
 324 50S to 500LS or SIPERNAT[®] D17 to D10, which are only differentiated by a grinding step, no
 325 improvements on flowability were observed.

326 To get a better look at these results, the SEM analysis of Avicel[®] PH-102 when adding 0.5% w/w
 327 of NPs is shown in figures 17, 18, 19 and 20. From SEM micrographs, it is possible to note that the
 328 VSSA values are not representative of the NM's size. Hydrophobic NPs (Figs. 19 and 20), with a
 329 smaller VSSA value, gave rise to smaller aggregates than the hydrophilic ones (Figs. 17 and 18).
 330 Bulk powder mixture with hydrophilic additives showed large aggregates/agglomerates (200 nm)
 331 adsorbed on the surface of the Avicel[®] PH-102 particles. In difference, Zimmermann et al. (2004)
 332 never found large agglomerates of fumed nano-silica adsorbed on the surface of the corn starch
 333 particles.

334 It should be expected that the particle/glidant bond strength influences the flow regulating potency
 335 of the NPs. The chemical treatment undergone to produce hydrophobic NPs decreases the number
 336 of hydrogen bonds. The lack of additional hydrogen bonds generates aggregates/agglomerates
 337 with an inferior bond strength, and so deagglomerate easily, thus giving rise to smaller aggregates.

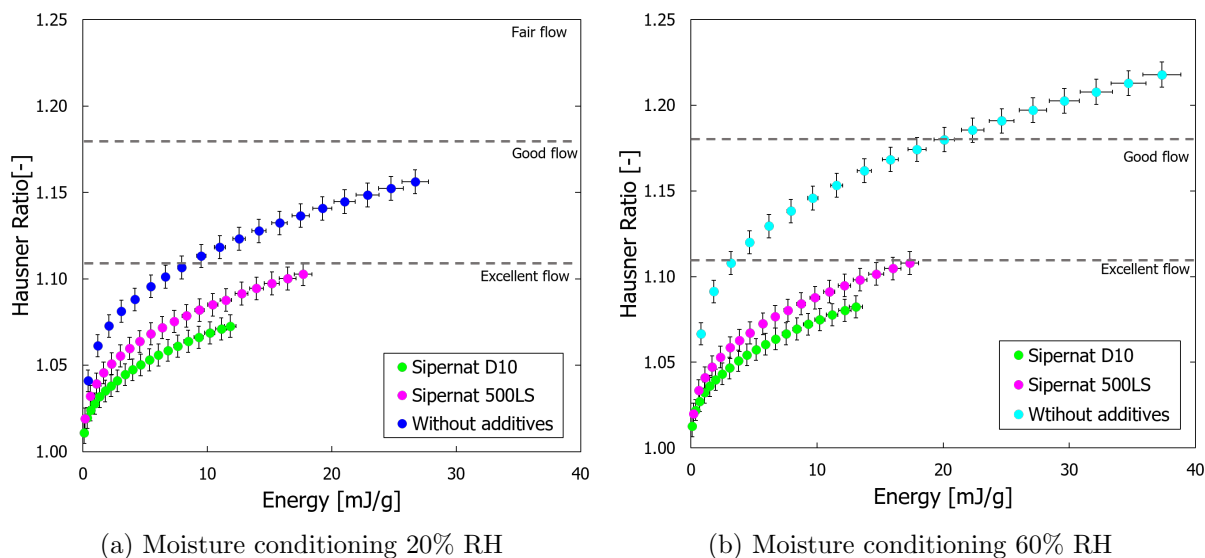


Figure 16: Influence of Sipernats D10 and 500 LS in the flowability of Avicel[®] PH-102. Mixtures prepared with 0.5% w/w of S-NPs and conditioned in different moisture environments.

338 This statement was validated in our study comparing figures 18 and 19. The smaller the NP
 339 aggregates the better the surface coverage.
 340

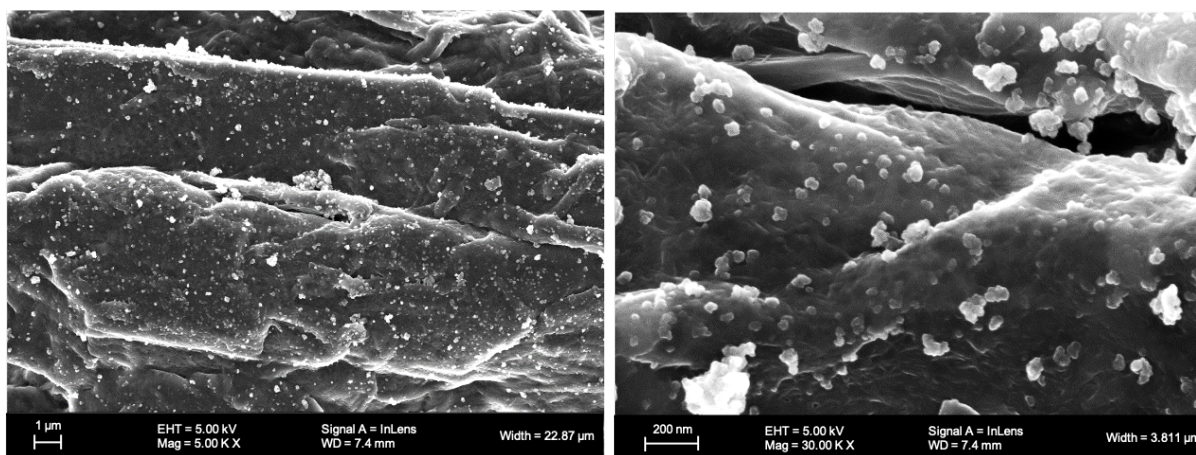


Figure 17: SEM micrographs of Avicel[®] PH-102 with 0.5% w/w of 50S, conditioned at 20% RH.

341 The flow regulating potency of the nano-additives also depends on the interparticle contacts:
 342 particle-to-particle, particle-to-silica, or silica-to-silica. This statement is related to the amount of
 343 NPs added to the mixtures using a relatively simple mathematical analysis (spherical monodisperse
 344 nanoparticles with random packing) like the one described by Valverde et al. (1998). In our case,
 345 we estimated that when adding 0.5 or 2% w/w of colloidal silica, the interaction between the grains
 346 is governed by silica-to-silica interactions. This rather rough estimation supports our results and
 347 could explain why no differences were found when increasing the amount of NPs added to the

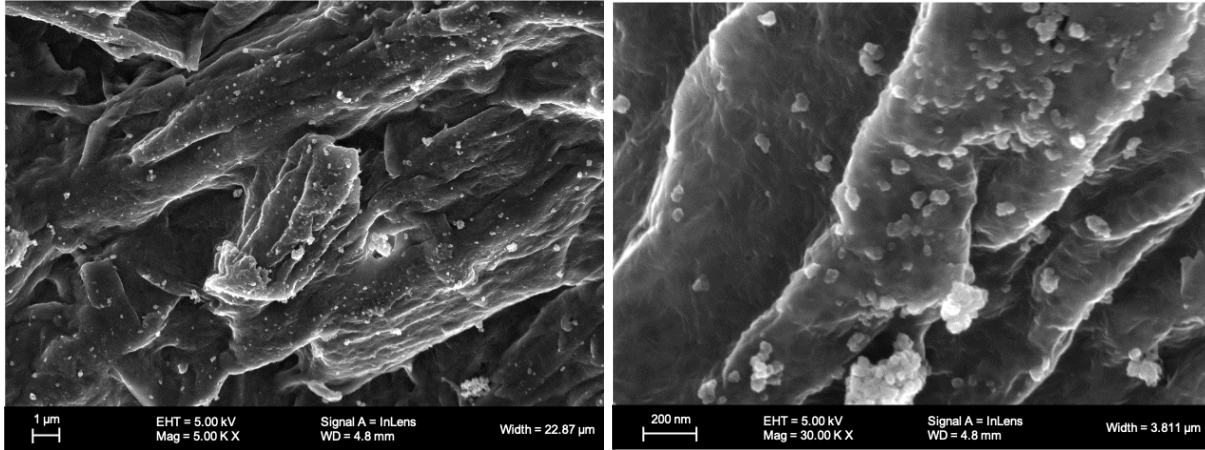


Figure 18: SEM micrographs of Avicel[®] PH-102 with 0,5% w/w of 500 LS, conditioned at 20% RH.

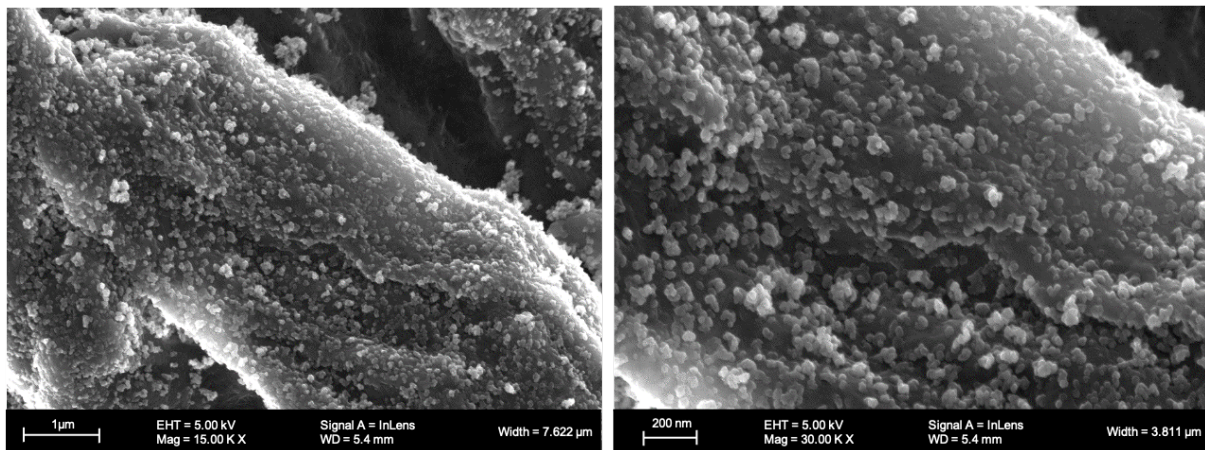


Figure 19: SEM micrographs of Avicel[®] PH-102 with 0,5% w/w of D10, conditioned at 20% RH.

348 mixtures, independently of their hydrophilicity (Figs. 15 and 16). All this somewhat rejects the
 349 assumption that the silica adsorbates lead to a flatter surface. Moreover, the change in the mixtures'
 350 surface chemistry, related to the glidants' hydrophilicity, improved flowability similarly, regardless
 351 of the moisture conditioning environment of the samples (Figs. 15 and 16). The mathematical
 352 approach also suggests that to cover the surface with 0.5% w/w, the adsorbates should measure
 353 300 nm. Nonetheless, Fig. 19 shows that binary mixtures with SIPERNAT[®] D10 generated a high
 354 coverage of particles with monodisperse fine adsorbates of around 50 nm.

355 When possible, surface coverage was also estimated using SEM micrographs using ImageJ software
 356 (Table 4). The number of adsorbates was determined in different regions of Avicel's surface of
 357 binary mixtures. For hydrophobic adsorbates, we obtained about 17% coverage for SIPERNAT[®]
 358 D17 and, at least, 80% for SIPERNAT[®] D10. For hydrophilic silica additives, a smaller surface
 359 area of the host particle was covered, from 6 to 16% for SIPERNAT[®] 500 LS and 50S, respectively.
 360 Even if this image analysis lacks statistical significance, it shows, and corroborates, that smaller

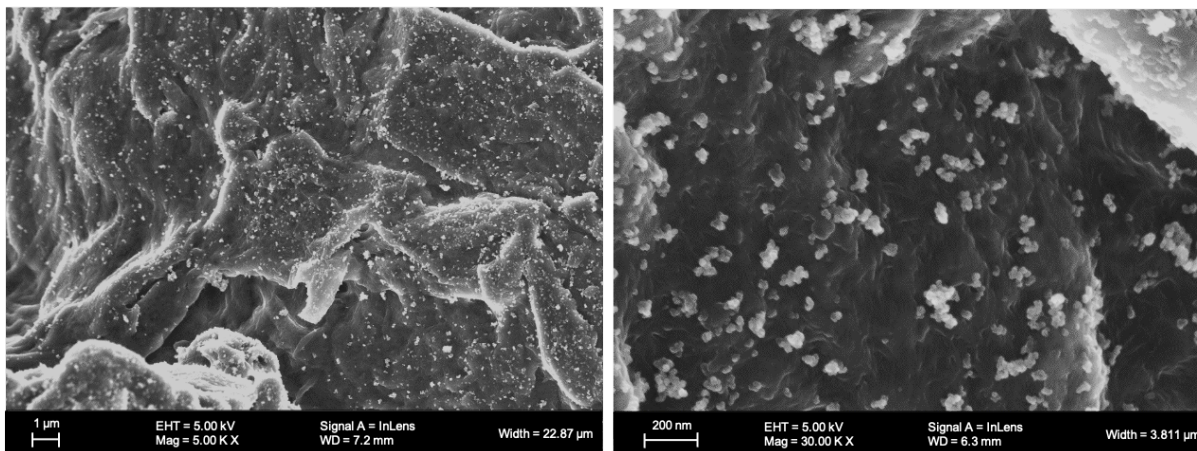


Figure 20: SEM micrographs of Avicel[®] PH-102 with 0,5% w/w of D17, conditioned at 20% RH.

361 adsorbates give rise to a better surface coverage, despite its hydrophilicity. It also highlights similar
 362 surface coverages with SIPERNAT[®] 50S and D17 binary mixtures, with a few bigger aggregates
 363 for 50S. Interestingly, although SIPERNAT[®] D10 produced a higher surface coverage, almost total
 364 (Fig. 19), flowability enhancement was obtained at lower surface coverages, similarly to when using
 365 SIPERNAT[®] D17.

366 In the literature, different surface coverage mass ratios, w/w, are proposed to improve
 367 flowability. Fulchini et al. (2017) found an optimum surface area coverage of around 20% w/w for
 368 mixtures of glass beads made cohesive by silanization. In their case, higher surface area coverages
 369 decreased flowability. According to Ruzaidi et al. (2017), for host particles with a mean diameter
 370 of 60 μm, the required amount of NPs to improve the powders' flowability is between 0.5 and 1%
 371 w/w. From our results, we can conclude that powder flowability improvement by glidants seems to
 372 be related to both of the following: nano-silica aggregate size distribution (obtained after mixing)
 373 and surface area coverage. We propose to define the amount of NPs to add to powder formulations
 374 in terms of surface coverage and not through mass ratios (w/w). A good example is proposed by
 375 Zhu et al. (2017). The authors determined by modeling the optimal size of nano additives and the
 376 minimal surface area coverage for binary mixtures of zeolite fine powder and nano-silica. It was
 377 suggested that, in order to reduce cohesiveness and to improve flowability, zeolite particles (0.5 -
 378 50 μm) should be covered with about 1% of 10 nm-additives.

Table 4: ImageJ software Analysis of SEM micrographs of Avicel[®] PH-102 surface in binary mixtures of 0.5% (w/w).

SIPERNAT [®]	Surface [μm^2]	Number of adsorbates [-]	Size of adsorbates [nm]	Coverage [%]
50 S	11	256	18 to 532	16
500 LS*	3.8	57	27 - 236	6
D17	9	214	17 to 316	17
D10 **			≤ 100	≥ 80

* low contrast

** naked eye

4 Conclusions

We have developed an experimental approach based on the energy supplied to powders during compaction under zero shear conditions. In these studies, we measured granular densification (bed height changes) as a function of the force applied to the system. Compaction is achieved during vertical tapping using Densitap and by subjecting the samples to low levels of stress during uniaxial compression using FT4. The compressibility of the powder bed was determined by the amount of energy supplied to the system during the test, but it could also be affected by the sample pre-consolidation state. We obtained a highly reproducible state by only conditioning the powder in a controlled moisture environment, thus validating the index choice.

Measurements were carried out to determine the moisture content's effect and the use of nanoparticles on the bulk flow properties of two well-known pharmaceutical excipients, Avicel[®] PH-102 and Retalac[®]. The influence of the moisture content influence was evaluated by conditioning the samples at 20 and 60% RH, while the impact of flow regulators impact was assessed by adding 0.5 and 2% w/w of precipitated silica nano-additives. From these measurements, we found an increase in flowability regardless of the glidant amount. Adding more silica from 0.5 to 2% w/w did not seem to reduce internal friction.

We also noted that all SIPERNAT[®] grades showed different levels of disaggregation. Surface coverage analysis showed that adding NPs reduced the size of the contact zone, thus decreasing particle-to-particle interactions, and so, cohesion. The hydrophilicity of the colloidal silica affected surface coverage. Binary mixtures with hydrophobic additives generated smaller silica aggregates that were better spread over the surface of the host particles, explaining its better performance. In conclusion, the improvement of powder flowability by flow additives seemed to be strongly related to both the surface area coverage, and the nano-silica aggregate size. We suggest choosing the type and the amount of nanomaterials to add to formulations by considering both the surface area coverage and the size of the flow regulators after mixing. These parameters somehow describe/determine the type of interactions or their transition: particle-to-particle, particle-to-silica, or silica-to-silica.

Finally, the dynamic of compaction of Avicel[®] PH-102 and Retalac[®] were fit by the Chicago

406 and the KWW model. Nonetheless, only the ρ -parameter (final compactness) from the Chicago
407 equation was correctly related to the steady state.

408 In conclusion, as a general trend, we suggest studying flowability from granular compaction
409 measurements by means of densification strength, related to the force or the energy supplied to the
410 media. An energetic approach shows and explains the differences in flowability assessment between
411 flow-testers. We have observed that device-related flowability agrees with the granular media flow,
412 as an observation, when determined at the densest compaction state.

413 5 Acknowledgements

414 This study is conducted in the framework of the "PowderReg" project, funded by the European
415 programme Interreg VA GR within the priority axis 4 "Strengthen the competitiveness and the
416 attractiveness of the Grande Region".

417 References

- 418 Duran Jacques (1997). *Sables, poudres et grains: introduction à la physique des milieux granulaires*.
419 Eyrolles sciences.
- 420 Fulchini, F., Zafar, U., Hare, C., Ghadiri, M., Tantawy, H., Ahmadian, H., and Poletto, M. (2017).
421 Relationship between surface area coverage of flow-aids and flowability of cohesive particles.
422 *Powder Technol.*, 322:417–427.
- 423 GDR MiDi (2004). On dense granular flows. *Eur. Phys. J. E.*, 14(4):341–365.
- 424 Head, D. A. (2000). Phenomenological glass model for vibratory granular compaction. *Phys. Rev.*
425 *E*, 62(2):2439–2449.
- 426 Knight, J. B., Fandrich, C. G., Lau, C. N., Jaeger, H. M., and Nagel, S. R. (1995). Density
427 relaxation in a vibrated granular material. *Phys. Rev. E*, 51(5):3957–3963.
- 428 Kojima, T. and Elliott, J. A. (2012). Incipient flow properties of two-component fine powder systems
429 and their relationships with bulk density and particle contacts. *Powder Technol.*, 228:359–370.
- 430 Majerová, D., Kulaviak, L., Ružička, M., Štěpánek, F., and Zámostný, P. (2016). Effect of colloidal
431 silica on rheological properties of common pharmaceutical excipients. *Eur. J. Pharm. Biopharm.*,
432 106:2–8.
- 433 Müller, A.-K., Ruppel, J., Drexel, C.-P., and Zimmermann, I. (2008). Precipitated silica as flow
434 regulator. *Eur. J. Pharm. Sci.*, 34(4):303–308.
- 435 Pharmacopeia, U. (2015). Bulk Density and Tapped Density of Powders.
- 436 Prescott, J. K. and Barnum, R. A. (2000). On powder flowability. *Pharm. Technol.*, 24(10):60–84.
- 437 Quintanilla, M. a. S., Valverde, J. M., and Castellanos, A. (2006). Adhesion force between fine
438 particles with controlled surface properties. *AIChE J.*, 52(5).
- 439 Rauscher, H., Roebben, G., Mech, A., Gibson, P., Kestens, V., Linsinger, T., and Reigo Sintes,
440 J. (2019). *An overview of concepts and terms used in the European Commission's definition of*
441 *nanomaterial*. Publications Office of the European Union.

- 442 Ribière, P., Philippe, P., Richard, P., Delannay, R., and Bideau, D. (2005). Slow compaction of
443 granular systems. *J. Condens. Matter Phys.*, 17:2743–2754.
- 444 Ricaud, M. (2007). Le point des connaissances sur les silices amorphes.
- 445 Rondet, E., Delalonde, M., Chuetor, S., and Ruiz, T. (2017). Modeling of granular material’s
446 packing: Equivalence between vibrated solicitations and consolidation. *Powder Technol.*,
447 310:287–294.
- 448 Ruzaidi, A. F. B., Mandal, U. K., and Chatterjee, B. (2017). Glidant effect of hydrophobic
449 and hydrophilic nanosilica on a cohesive powder: Comparison of different flow characterization
450 techniques. *Particuology*, 31:69–79.
- 451 Saker, A., Cares-Pacheco, M. G., Marchal, P., and Falk, V. (2019). Powders flowability assessment
452 in granular compaction: What about the consistency of Hausner ratio? *Powder Technol.*, 354:52–
453 63.
- 454 Schulze, D. (2008). *Powders and Bulk Solids: Behavior, Characterization, Storage and Flow*.
455 Springer-Verlag, Berlin Heidelberg.
- 456 Traina, K., Cloots, R., Bontempi, S., Lumay, G., Vandewalle, N., and Boschini, F. (2013). Flow
457 abilities of powders and granular materials evidenced from dynamical tap density measurement.
458 *Powder Technol.*, 235:842–852.
- 459 Valverde, J. M. (2013). The Use of Additives to Control Powder Flow. Mechanical Properties of
460 Fine Powder Beds. In *Fluidization of Fine Powders: Cohesive versus Dynamical Aggregation*,
461 Particle Technology Series, pages 99–120. Springer Netherlands, Dordrecht.
- 462 Valverde, J. M., Ramos, A., Castellanos, A., and Keith Watson, P. (1998). The tensile strength
463 of cohesive powders and its relationship to consolidation, free volume and cohesivity. *Powder
464 Technol.*, 97(3):237–245.
- 465 Yu, A. B. and Hall, J. S. (1994). Packing of fine powders subjected to tapping. *Powder Technol.*,
466 78(3):247–256.
- 467 Zhu, X., Qiang, Z., Huang, C., Wang, Y., and Wei, F. (2017). Validation of surface coating with
468 nanoparticles to improve the flowability of fine cohesive powders. *Particuology*, 30:53–61.
- 469 Zimmermann, I., Eber, M., and Meyer, K. (2004). Nanomaterials as Flow Regulators in Dry
470 Powders. *Z. Phys. Chem.*, 218(1):51–102.